Journal of Structural Geology 33 (2011) 743–755

Contents lists available at ScienceDirect

Journal of Structural Geology

journal homepage: www.elsevier.com/locate/jsg

Structure and Holocene evolution of an active creeping thrust fault: The Chihshang fault at Chinyuan (Taiwan)

Chung-Hsiang Mu [a,b], Jacques Angelier [b], Jian-Cheng Lee [c,*], Hao-Tsu Chu [d], Jia-Jyun Dong [a]

[a] Graduate Institute of Applied Geology, National Central University, No. 300, Jhongda Rd., Jhongli City, Taoyuan County 32001, Taiwan, ROC
[b] Observatoire de la Côte d'Azur and Observatoire Océanologique de Villefranche, Géosciences Azur, La Darse, B.P. 48, 06235, France
[c] Institute of Earth Sciences, Academia Sinica, P.O. Box 1-55, Nankang, 128, Sec. 2 Academia Road, Taipei 11529, Taiwan, ROC
[d] Central Geological Survey, Taipei, Taiwan, ROC

ARTICLE INFO

Article history:
Received 11 September 2009
Received in revised form
28 January 2011
Accepted 29 January 2011
Available online 18 February 2011

Keywords:
Creeping fault
Active thrusting
Fault geometry
Sedimentation and tectonics
Geodetic measurement
Kinematic analysis

ABSTRACT

We conducted a variety of measurements and analyses at Chihshang Active Fault Observatory in eastern Taiwan, including surface-rupture mapping, three shallow borehole core analysis and kinematic analysis of geodetic measurements. We found that the Chihshang fault exhibits a three-branch fault system in the Chinyuan alluvial fan, which is composed of at least 100 m thick gravel deposits. Outside of the Chinyuan River, the Chihshang fault shows a single fault system with a sharp lithological contact. Combining the leveling results and trench excavation, we interpret that the three fault branches are coupled with a 50–60-m-wide pop-up structure in the hangingwall. Based on the ratio between vertical and horizontal displacements, we obtained dip angles of 38°, 62° and 16° for two west-vergent thrusts and an east-vergent backthrust, respectively. This pop-up was estimated to develop at the uppermost 30–40 m unconsolidated gravels during the last few thousand years above the main fault with a dip angle of 42°. By compiling the available ages data, we obtained an uplift rate of 2.3 cm/yr of the Chihshang fault and an alluvial sedimentation rate of 1.1 cm/yr during the past thousands years. Consequently, the individual uplift rate for each fault branch at the Chihshang Observatory was slightly less than the deposition rate of the Chinyuan River. No geomorphic fault scarp can thus be observed in the three-branch fault system area.

1. Introduction

Behaviour of active faults generally can be divided into two distinct periods during an earthquake cycle: earthquake slip and interseismic slip or lock. Study of active faults provides insights about the seismological characterization of faults, including the state of strain accumulation on faults (Thatcher, 1984), recurrence time of earthquakes (Sieh and Williams, 1990), long-term slip model (Sieh et al., 1989), and so on. On the one hand, geodetic data, such as GPS, leveling, etc., provides short-term surface-deformation rates associated with the active fault movement. On the other hand, near-surface fault zone character, such as stratigraphy, geological structures, and fault geometry, also help to delineate the fault kinematics and slip behaviours on a fault near the surface in a geological time scale. The Chihshang fault in eastern Taiwan has exhibited both types of active fault movements during the past 60 years: two moderate to large earthquakes separated by 52 years and rapid interseismic creep in the intervals. The Chihshang thrust fault is one of the most active segments of the Longitudinal Valley fault (LVF), which is located along the plate suture between the Philippine Sea and the Eurasian plates in eastern Taiwan (Ho, 1986; Tsai, 1986; Angelier, 1986; Angelier et al., 1997; Fig. 1).

Tectonically, the Coastal Range of the Luzon arc obliquely attached to the Chinese continental margin in eastern Taiwan along the LVF. The N20°E-trending, 35-km-long Chihshang fault closely follows the conspicuous morphological feature that marks the boundary between the Coastal Range and the valley in the middle-southern part of the Longitudinal Valley (Fig. 1c). At the surface, the Lichi Mélange represents the geological strata in the hangingwall and is thrust over on the flat late Quaternary alluvial deposit of the Longitudinal Valley (Fig. 1d). The Lichi Mélange, which is composed of strongly sheared chaotic mudstones and the exotic blocks of various lithologies, such as ophiolitic suite, sedimentary deposits, and andesitic volcanic rocks, was a subduction product formed from the accretionary wedge between the subducting South China Sea oceanic slab and the overlying Luzon volcanic arc during Mio-Pliocene time (Biq, 1973; Ernst, 1977; Teng and Wang, 1981; Page and Suppe, 1981; Barrier and Muller, 1984; Hsu, 1988; Chen, 1991, 1997; Chang et al., 2000; Huang et al., 2007).

* Corresponding author.
E-mail address: jclee@earth.sinica.edu.tw (J.-C. Lee).

0191-8141/$ – see front matter © 2011 Elsevier Ltd. All rights reserved.
doi:10.1016/j.jsg.2011.01.015

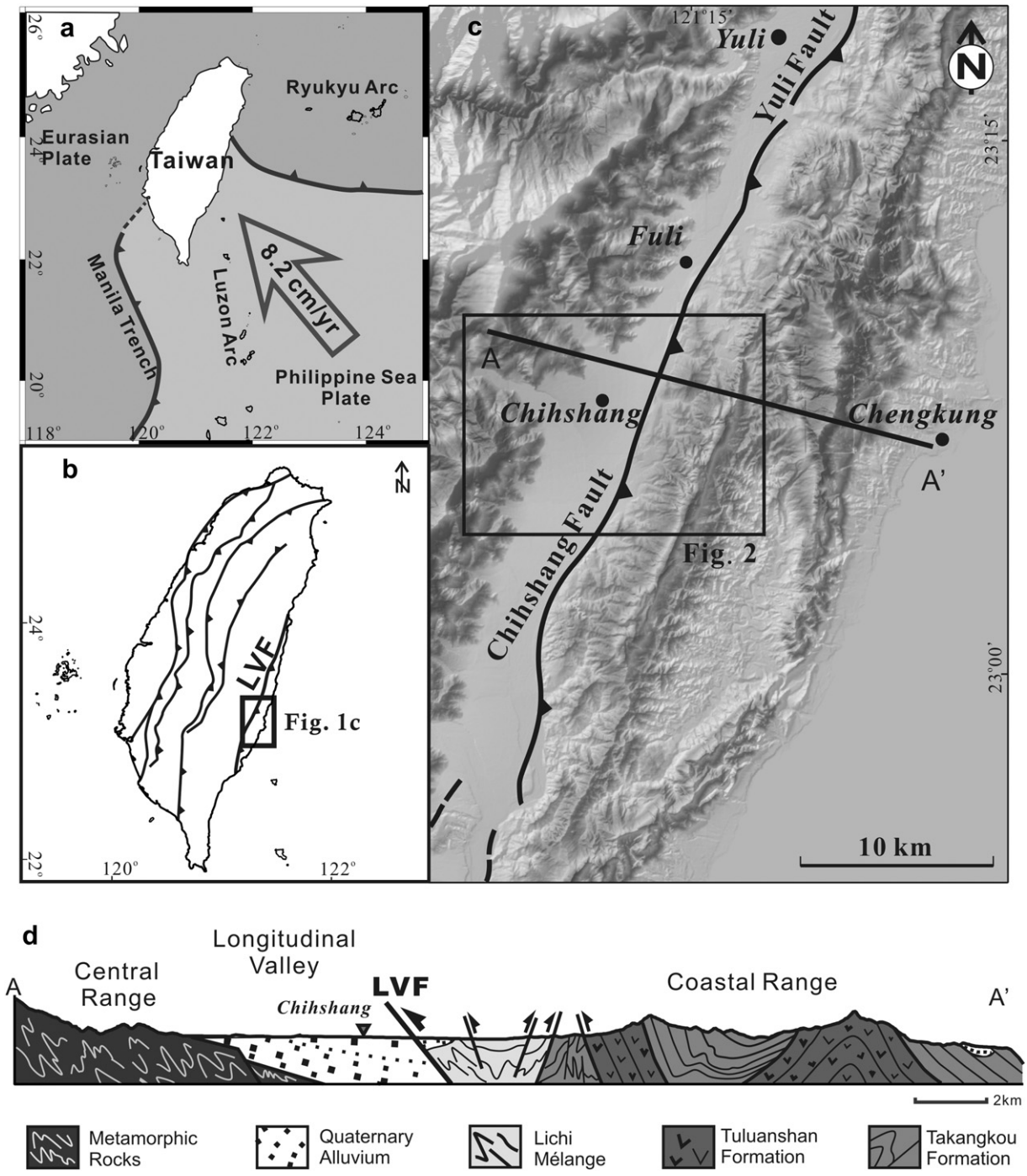

Fig. 1. Tectonic and geological setting of study area. (a) Map of simplified plate tectonic setting. (b) Major faults in the Taiwan island. The Longitudinal Valley fault, LVF, represents the present plate suture. (c) The topography along the 35-km-long Chihshang fault. (d) Geological cross-section near Chihshang.

The 1991–1996 GPS measurements showed that the Philippine Sea plate was moving north-westward at a rate of 8.2 cm/yr relative to the Chinese continental shelf of Eurasia in the Taiwan area (Yu et al., 1997). Two historical, large earthquakes that ruptured the Chihshang fault in the last 60 years: the Ms = 6.2 Chihshang earthquake in 1951 (Hsu, 1962; Cheng et al., 1996) and the Mw = 6.8 Chengkung earthquake in 2003 (Chen et al., 2006; Lee et al., 2006; Wu et al., 2006; Kuochen et al., 2007; Hu et al., 2007; Hsu et al., 2009). The seismological analysis of the 2003 Chengkung earthquake sequence revealed that the Chihshang fault has a listric-shape geometry, with a relatively steep dip angle of 50–70°E at the depth of 0–15 km below the Coastal Range, gradually turning into a gentler dip of 15–30°E at the depth of 20–25 km off the eastern coast of Taiwan (Lee et al., 2006; Hu et al., 2007; Kuochen et al., 2007). Between these two large earthquakes, a variety of on-site measurements of displacement have been undertaken across the Chihshang fault during the last 30 years. They include campaigned surveys (i.e., GPS surveys, trilateration networks, leveling, nail networks) and permanent geodetic stations (i.e., creep meters monitoring and continuous GPS stations) (Yu and Liu, 1989; Yu et al., 1990, 1997; Angelier et al., 1997, 2000; Yu and Kuo, 2001; Lee et al., 2001, 2003, 2005 and 2006) (Fig. 2). The measurements

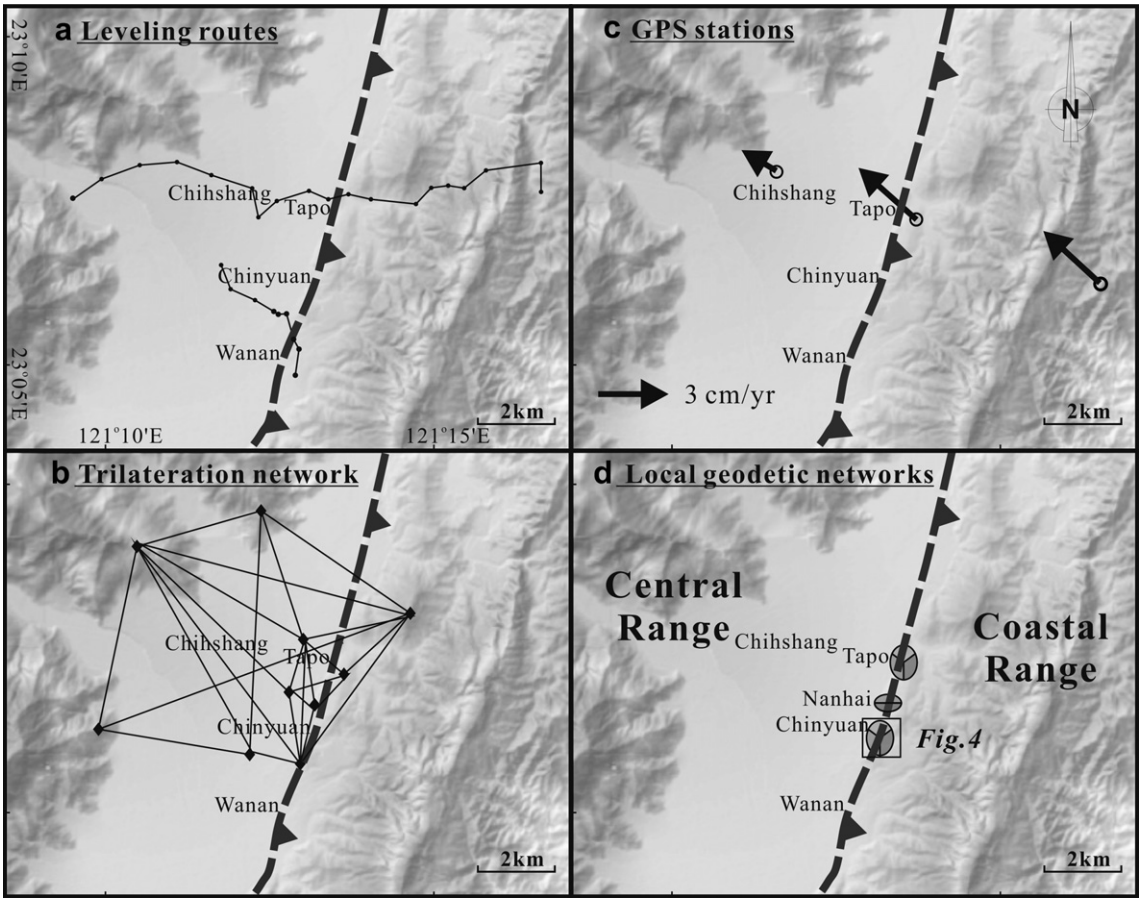

Fig. 2. Geodetic measurements along in the Chihshang area during the last 30 years. (a) The 1983–1988 leveling routes (data from Yu and Liu, 1989). (b) The 1983–1988 trilateration network (from Yu and Liu, 1989). (c) Three campaigned GPS stations across the Chihshang fault (Yu and Kuo, 2001). (d) Three local near-fault geodetic networks: (1) Tapo site including two creep meters, trilateration networks, GPS measurement, and leveling routes, (2) Nanhai site including trilateration networks, GPS measurement, and leveling routes, and (3) Chinyuan site including trilateration networks, GPS measurement, leveling routes, and three creep meters (see the detailed map in Fig. 4).

revealed rapid interseismic creep with 2–3 cm/yr horizontal shortening in the N310°E direction across the Chihshang fault and that the surface-deformation limited to a narrow fault zone, ranging from a few tens to few hundred meters in width. The measurements also indicated that the interseismic deformation on the Chihshang fault accounted for 35–40% of the total plate convergence (Lee and Angelier, 1993; Angelier et al., 2000).

Although both the coseismic slip and interseismic creep of the Chihshang fault are relatively well studied and the surface trace of the fault is mostly well defined, the subsurface fault zone structures, in particular the distribution of the branches and their geometry remained little known. Recently, an interdisciplinary project was conducted to better understand the geometry and recent movements of the Chihshang fault, including repeated geodetic measurements across the fault zone, core-drilling boreholes, groundwater table monitoring, paleoseismological trenches, seismometers recording, seismic reflection profiles, and electric resistivity survey. In this paper, we use results from this interdisciplinary study to focus on reconstructing the fault zone geometry at the shallow level and to characterize the kinematics of the fault slip and Holocene evolution of the fault with relation to the rapid fluvial deposition along the fault.

2. The Chihshang active fault observatory

We first describe briefly different geodetic surveys, which were conducted along the Chihshang fault zone, including at the 'Chihshang Active Fault Observatory' near Chihshang town (Fig. 2) during the past 30 years. In 1983–1988, two leveling routes (Fig. 2a) and a trilateration network (Fig. 2b) in Chihshang were repeatedly surveyed on an annual basis (Yu and Liu, 1989). The results indicated that the horizontal shortening rate and the relative uplift rate across the Chihshang fault were 2 cm/yr and 1.9 cm/yr, respectively. Since 1990, repeated on-site measurements of the surface fractures (1–2 times annually), based on direct measurement and nail networks implanted on the retaining walls, were conducted at 4 different sites between Tapo and Wanan villages (Chu et al., 1994; Lee, 1994; Angelier et al., 1997, 2000). The results showed that the relative displacement vector across the Chihshang fault trends N48°W on average, with a shortening rate of 2.7 cm/yr in 1990–1995. In 1998–1999, Lee et al. (2001, 2006) installed five creep meters straddling the surface fractures in the fault zone, and installed near-fault local geodetic networks for repeated measurements, including trilateration measurements, GPS, and leveling surveys, at 4 sites at the scale of a few hundred meters wide across the fault (Fig. 2d). The combining results of the above geodetic on-site measurement at the Chihshang fault revealed a steady creep rate of 2.2–2.5 cm/yr in 1988–1998 (Fig. 3), which interestingly decreased to 1.5–1.8 cm/yr in 2000–2003, a few years before the 2003 Mw = 6.8 Chengkung earthquake, then returns to a steady creep rate of 2.0 cm/yr since 2007 (Fig. 3b).

The coseismic slip of the Chengkung earthquake and the subsequent post-seismic creep at the near surface of the Chihshang fault in Chihshang Observatory combined for about 14 cm of total horizontal shortening and 15 cm of vertical displacement across the

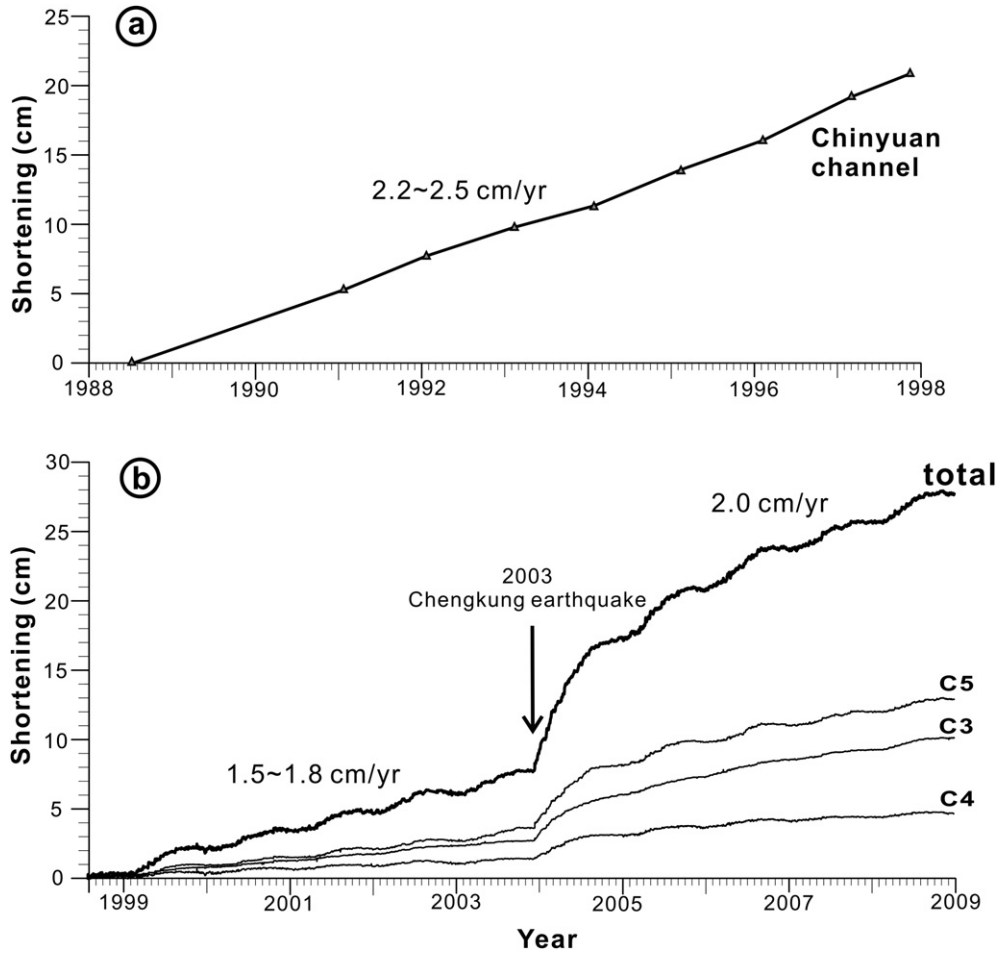

Fig. 3. Evolution of shortening on the three branches of the Chihshang fault at Chinyuan from 1988 to 2009. (a) Result of nail network measurement from 1988 to 1998, indicating an average shortening velocity of 2.2–2.5 cm per year for total shortening of the three branches (Angelier et al., 2000). (b) Shortening from 1998 to 2009, from daily creep meter records (Lee et al., 2003, 2006; this paper for 2007 to the end of 2009). The wave-shaped shortening curve reveals a seasonal variation in shortening magnitude. Note that the 2003 Mw6.8 Chengkung earthquake produced a smaller coseismic shortening and a relatively larger post-seismic shortening. See detailed descriptions in the text.

surface fault zone from December 2003 to the end of 2006 (Fig. 3b). Furthermore, the creep meters measurements recorded a small coseismic slip of less than 1–2 cm as compared to later post-seismic creep, which is interpreted to indicate that during the earthquake, coseismic slip did not propagate effectively to the near surface in the alluvial deposits (Lee et al., 2006; Chang et al., 2009). The cause of this behavior was interpreted as frictional instability due to visco-elastic behaviour of the thick unconsolidated late-Quaternary deposits in the footwall of the Chihshang fault (Lee et al., 2006; Chang et al., 2009).

Interestingly, the creep meters data at Chihshang Observatory show that fault creep varies seasonally (Lee et al., 2003, Fig. 3b), which is interpreted to result from locking of the fault slip at shallow depth during the dry season. Consequently, near-surface fault motion relates to rainfall or groundwater table variations, probably via effects on the near-surface mechanical properties, in particular friction of the fault zone (Lee et al., 2006). This interpretation is consistent with the modeling work of Chang et al. (2009) using frictional instability law (Marone et al., 1991; Perfettini and Avouac, 2007) together with 1-D hydraulic diffusion model for the Coulomb-rupturing criteria to suggest that the seasonal lock-and-creep of the Chihshang fault is restricted to the upper 500–600 m of the crust. As a result, the subsurface geological structure of the Chihshang fault is important to understand at the near-surface level. Although the recent displacement history along the Chihshang fault is documented, much less is known about the shallow structure of the fault zone. However, the Observatory provides an exceptional opportunity to investigate this subsurface geological structure given the variety of data sets.

In this study, we drilled three shallow boreholes with core sampling (T1, T2, and T3) in 2006–2007 at the Chinyuan site (Fig. 4) to penetrate the primary fault at the shallow level. Rotary drilling was used for core sampling with a core diameter of 10.1 cm (i.e., 4 inch). The extraction percentages of core exceeded 90% for all three boreholes. 500 m farther south, three boreholes (Wan-1, Wan-2, and Wan-3) were drilled by the Central Geological Survey (Chen, 2009) to penetrate the main fault zone, also providing valuable data for reconstructing the geological structures of the Chihshang fault. In addition, three trenches for a paleoseismology investigation were excavated by the National Taiwan University and Central Geological Survey at the Chinyuan site (Chu, 2007). The results also provided helpful information about near-surface stratigraphy and structure across the fault zone.

3. Geological reconstruction of the fault architecture

3.1. Mapping the surface branches of fault

Along the Chihshang fault, man-made structures show widespread brittle deformation structures, providing a good opportunity

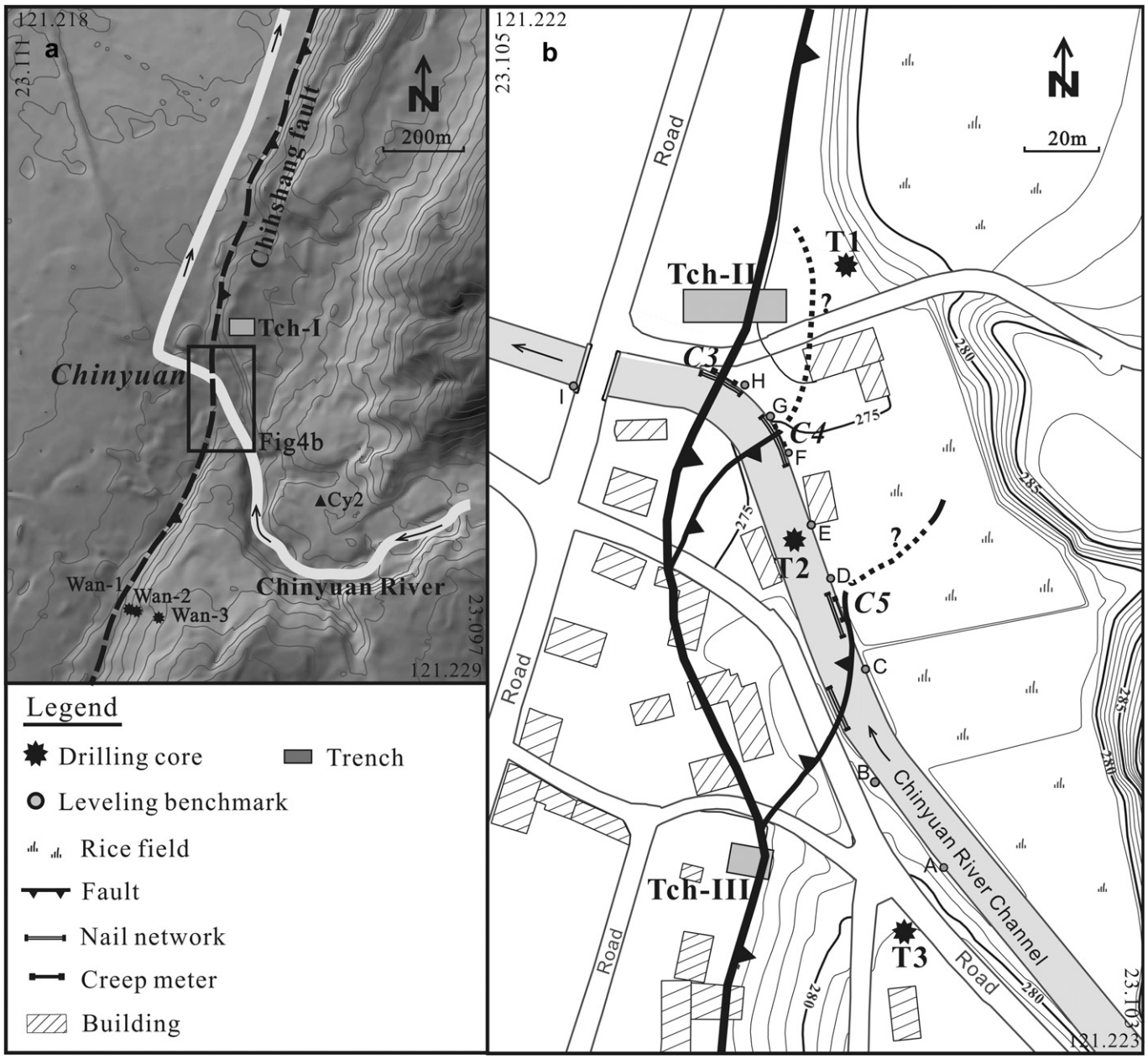

Fig. 4. Map of surface branches in the Chihshang active fault Observatory. (a) Location of the Chihshang Observatory and related work sites around the Chinyuan site. (b) Mapped surface faults at the Chinyuan site. Topography was measured and revealed by 1-m contour lines. A variety of instrumentation was conducted at the Chinyuan site, including leveling, creep meters, GPS, boreholes and trenching, as shown by symbols and letters in the map. See details in the text.

to reconstruct and quantify fault movement (e.g., Angelier et al., 1997). For example, the concrete riverbanks in Chinyuan contain exposures of three fracture zones (Fig. 4b). These three fault branches continue into the Chinyuan village with numerous fractures in the houses and ground. The three fault branches from west to east are respectively two west-verging, east-dipping faults (C3, C4, Fig. 5a and b) and an east-verging, west-dipping fault (C5, Fig. 5c and d). We interpret the westernmost branch (C3) as the primary fault, because it follows the major geomorphic scarp in and around the Chinyuan village closely. Furthermore, the other two branches are difficult to trace in the northern part of the alluvial fan due to poor exposure in rice paddies. The three fault branches in the retaining walls are interpreted as thrust faults according to the results of on-site geodetic network measurements (Lee et al., 2006). During the 2003 Chengkung earthquake, each branch had a few mm of coseismic displacement, which is interpreted to confirm their connection to the main fault at depth.

3.2. Boreholes core analysis

3.2.1. Three cored boreholes at Chinyuan (T1, T2, T3)

The 60-m-deep T1 is located in the hangingwall about 20–25 m east of the scarp of the main fault (Fig. 4). Core skins were scratched at laboratories to better observe the compositions, and stratigraphic and tectonic structures.

From 0 m to 17 m of depth, the sediments are alluvial deposits mostly composed of clay and sand (Fig. 6), which we interpret as overflow fine-grained deposits of the Chinyuan River mixed with colluvium from nearby. Below 17 m, the core is composed of coarse gravel with coarse sand matrix. The composition of the gravel

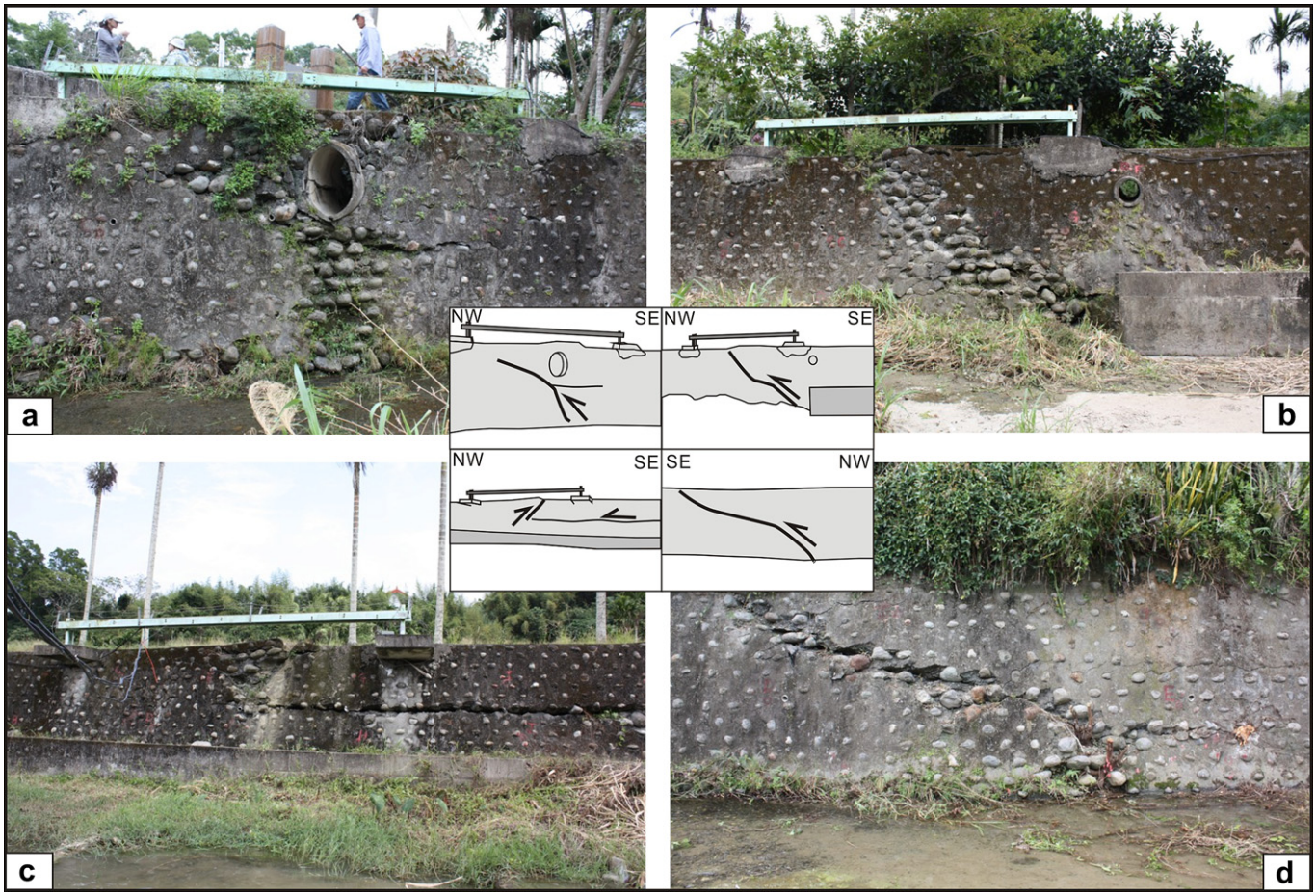

Fig. 5. Field photographs of the three branches faults on the retaining wall of the river channel in Chinyuan. (a) W-verging frontal fault at creep meter C3. (b) W-verging middle fault at creep meter C4. E-verging upper, backthrust fault at creep meter C5 (c) and on the opposite side of channel (d). Note that the actual W-dip direction of this upper fault is directly observable in (d), whereas (c) shows an apparent E vergence that results from the presence of a near-surface "crocodile mouth" structure at the level of the channel bottom.

varies, including andesitic volcanic rocks and sedimentary rocks that represent typical rock lithologies from the Coastal Range. Below 48 m, the sediment is a mix of metamorphic quartz grains and volcanic rocks with coarse sand matrix. The compositions represent the rock lithologies mixed from both Central Range and Coastal Range. Three fault zones have been observed in T1 60-m-long core at 12.8, 14.5–15.6 and 36.4 m depth (Fig. 6). The uppermost fault shows striated shear planes with a fault dip angle of 45°–50°. The middle fault has a dip angle of 50°. The lowermost fault is a shear surface of dipping angle of 30°. These faults are interpreted to be diffusely distributed branches of the Chihshang fault in these unconsolidated sediments.

The 60-m-long T2 borehole was drilled under the concrete pavement of the Chinyuan River channel, about 35–40 m east of the surface breaks of the primary fault (Fig. 4). The T2 core is mainly composed of gravel deposits, except the upper 10 m with sand and occasional clay layers (Fig. 6). From 10 m to 45 m depth, the gravels contain clasts of andesitic volcanic rocks, igneous rock and coarse sand matrix with metamorphic quartz, which are consistent with possible source rocks of both the Coastal Range and the Central Range. From 45 m to 60 m depth, the gravels are mainly composed of andesitic volcanic rocks. We found larger size of gravels and coarser matrix compared with the other boreholes, which is consistent with the fact that the T2 is situated in the middle of the fluvial channel of the Chinyuan River. Four faults were observed in the core: (1) the upper three are located at depths of 12.5 m, 21 m and 26.5 m, with similar dip angles of 50°–60°; and (2) the lowest one occurs at 45 m, with a gentler dip of 35°.

The 100-m-long core T3 is located outside of three-branch-fault system in Chinyuan alluvial fan and is about 40 m east of the surface scarp of the primary fault (Fig. 4). The core is composed mainly of gravels with a matrix of fine-grained sand to silt. The composition of gravel clastic varies, including andesitic volcanic and metamorphic rocks. We distinguished the gravels layers into two facies: the upper 42–44 m is mainly composed of a mix of volcanic rocks, quartz pebbles and metamorphic fragments; whereas the lower part is mainly composed of andesitic gravels. As a result, we interpret the lower gravels as ancient fluvial or alluvial fan deposits of the Chinyuan River and the upper 42–44 m as fluvial deposits of the river flowing along the Longitudinal Valley. Two sharp faults with striations occur at 54 m and 90 m depths.

Combining the locations of the faults observed in the above three cores, we tried to reconstruct the subsurface fault structure, including the three fault branches geometry and distribution of fault zone. Using simple near-continuous subsurface projections, we interpret that (1) the main fault connects the surface fault of C3, the fault at 12.8–15.6 m of the core T1, and the fault at 21–26.5 m of T2; (2) the branch of the surface fault C4 connects with the fault at 12.5 m of T2. As a result, the geometry of the main fault zone has a dip of 30°–40° toward the east and the middle branch fault has a dip of 50°–60° (Fig. 7a), for the three-branch system in the Chinyuan alluvial fan. As for profile across the southern part of the Chinyuan site where only a single fault is present, we connected the

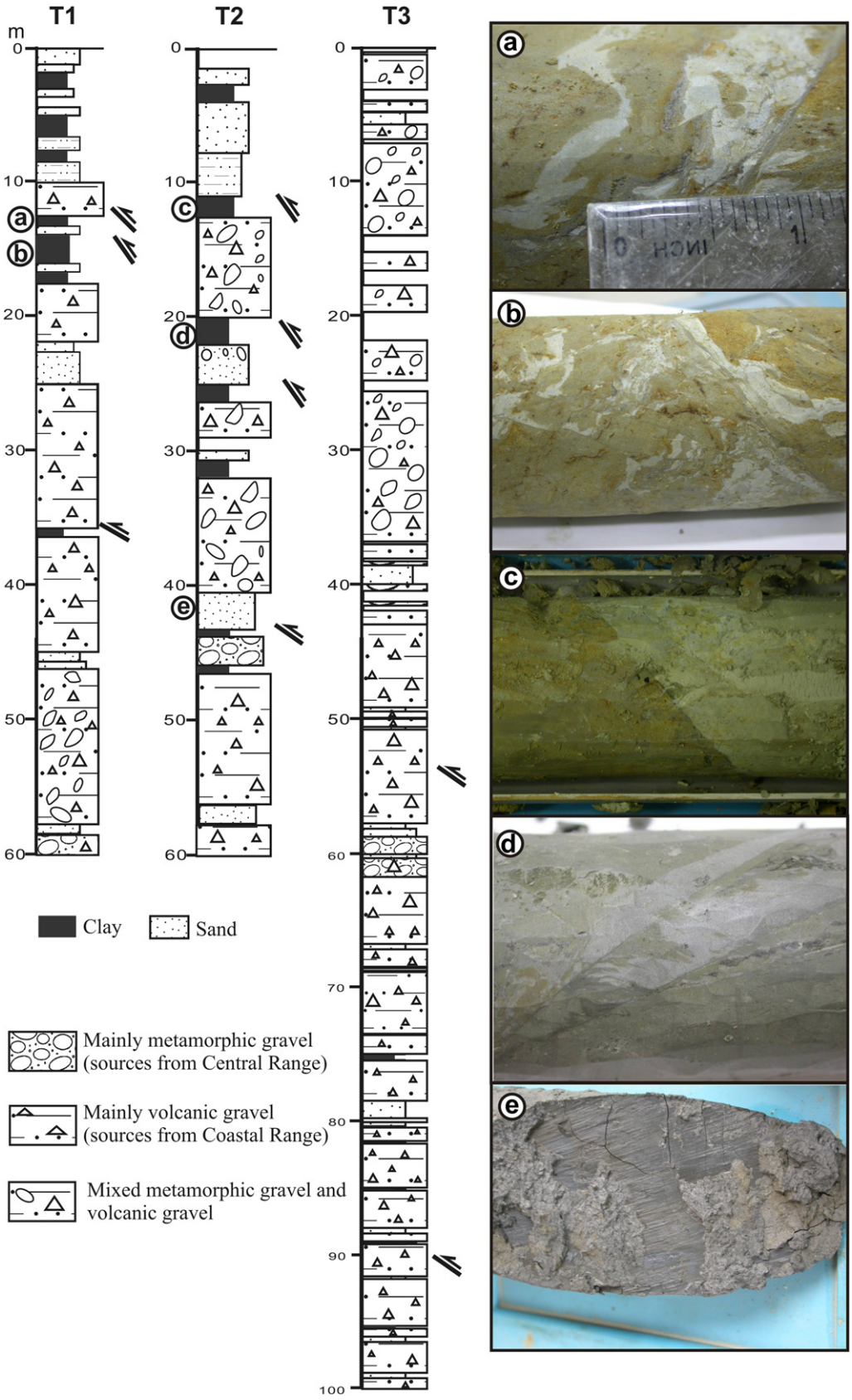

Fig. 6. Core logs for wells T1, T2 and T3 with lithological facies and fault zones at Chinyuan (location in Fig. 4). The photographs on the right illustrate the characteristics of the fault zones in the cores (letters key photos to positions in boreholes on left). (a) Fault zone at 12–13 m depth of T1. (b) Fault zone at 14–15 m depth in T1. (c) Fault at 11–12 m depth in T2, showing typical striated fault surface in mud layers. (d) Fault at 20–21 m depth in T2 with intercalation of sand and mud layers and a fault dip angle of about 40–50°. (e) Slickenside in the mud layer.

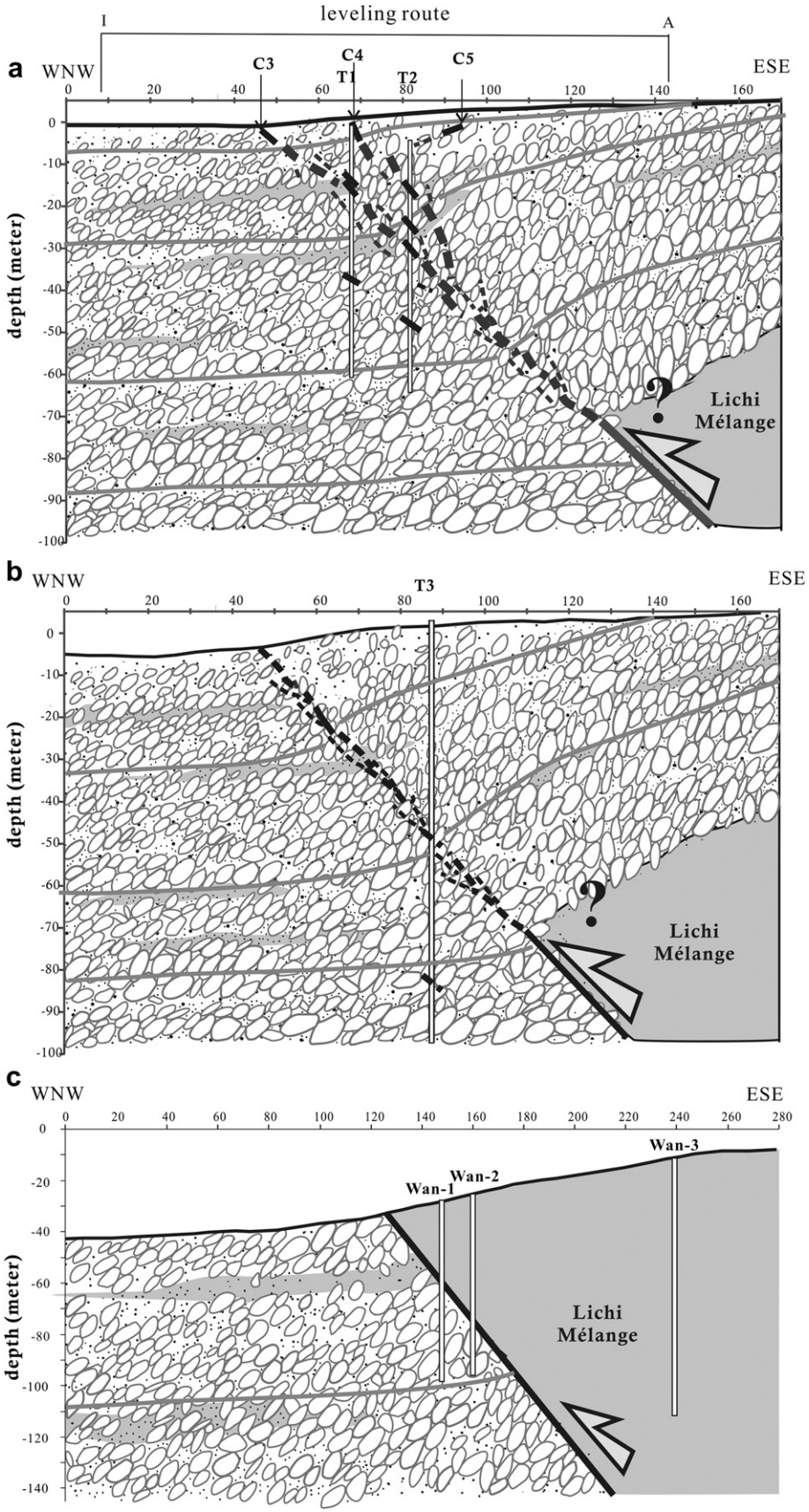

Fig. 7. 2-D schematic geological cross-section with fault architecture of the Chihshang fault in the near surface at three different locations. (a) Chinyuan site I, within the alluvial fan of the Chinyuan River, showing a diffused fault zone with a three-branch fault system in the upper 30–40 m. (b) Chinyuan site II, outside of the Chinyuan River channel, showing a single-fault system with a diffused fault zone in the upper unconsolidated deposits. (c) Wanan site, characterizing by a sharp fault zone separating the Lichi mélange to the hangingwall and alluvial deposits to the footwall.

surface fault scarp to the fault at 54 m at the core of T3 to obtain a dip of 45°–50° (Fig. 7b). Based on the observations from the cores and the trenching excavated cross sections at the Observatory (Chu, 2007), the fault zone is generally composed of several faults in a diffused zone instead of a sharp fault plane, which is consistent with our interpretation from core analysis. This outcome is not surprising, considering the facts that the fault is developing within young unconsolidated gravel deposits, which are quite inhomogeneous with relatively hard pebbles surrounded by much softer sand/mud matrix.

3.2.2. Three boreholes in Wanan

In addition to our three boreholes, we examined three nearby boreholes drilled by Central Geological Survey and National Taiwan University (Chen, 2009), about 500 m south of the Chinyuan site in Wanan (Fig. 4a). These three boreholes, Wan-1, Wan-2 and Wan-3, were drilled along a 150-m-long line perpendicular to the strike of the Chihshang fault. Unlike the Chinyuan site, fluvial deposits are absent from the hangingwall in the Wanan site, whereas the Lichi Mélange is present. The 70-m-long core of Wan-1, drilled in the hangingwall about 25 m east of the fault scarp showed that the main fault plane is located at the depth of 29 m with l-m-thick fault gouge. The main fault separates the Lichi Mélange in the hangingwall from recent alluvial gravels intercalated with fine-grained sand/silt in the footwall (Fig. 7c). The 70-m-long core of Wan-2, drilled about 40 m east of the fault scarp, revealed a similar fault zone at the depth of 46.4 m juxtaposing hangingwall the Lichi Mélange from the recent alluvial deposits to the footwall. The 100-m-long Wan-3 core in the hangingwall and 150 m from the fault scarp exclusively contained the Lichi Mélange and no occurrence of the fault zone. Combining the information from the three boreholes in Wanan, the Chihshang fault has a dip angle of 45–50° at a shallow depth in this area (Fig. 7c).

3.2.3. Summary and geological implications

The drilling results reveal that the dip angle of the Chihshang fault is approximately 30–40° within the Chinyuan alluvial fan with three-branch system and 48° outside of the fan in Chinyuan and Wanan. Also, the juxtaposed stratigraphic units and the implications for the proximity of deposition adjacent to the fault differ between Chinyuan and Wanan. At Wanan, the fault has a distinct zone and the hangingwall is almost exclusively composed of the mudstone of the Lichi Mélange. Whereas at Chinyuan, a large accumulation of river sediments of gravels of the present Chinyuan River occupies greater than 100 m of the hangingwall, plus no distinct fault zone is present and instead, the fault is inferred to be distributed into a diffused zone with particular fault planes occurrences based on dip projection. Long-term geologically speaking, the Lichi Mélange represents the main rock formation on the hangingwall of the Chihshang fault against the late-Quaternary deposits on the footwall. On top of the Lichi Mélange and near the fault, Holocene fluvial and alluvial deposits can be commonly observed. At the Observatory of Chinyuan site, it represents a case where the Lichi Mélange has been eroded and covered by alluvial deposits, mainly due to the stream power of the Chinyuan River, which flows from the Coastal Range to the valley. As a consequence, the Observatory illustrates a particular case, where the Holocene unconsolidated alluvial deposits occupy the hangingwall near the fault instead of the Lichi Mélange.

The leveling measurements at the Chinyuan site in 1998–2006 (Lee et al., 2006) exhibit an arched form of vertical deformation in the hangingwall compared to little vertical movement in the footwall (Fig. 8), which is consistent with ongoing anticlinal folding (i.e., a pop-up structure) between C3 fault and C5 fault. Furthermore, a 50-m-long, 5-m-deep trench excavation at the same location in 2004 showed the forelimb of a gentle anticline in the subsurface strata near the primary fault surface trace (Chen, 2009). Combining these data, we interpret the presence of an about 100-m-wide anticline above the main fault at the Chinyuan site (Fig. 7a and b).

4. Geodetic analysis and fault kinematics

Assuming that the Chihshang fault splits into three branches with fractures zones in the Chinyuan village, the three creep meters, straddling the faults, provide detailed records of their movements (Lee et al., 2003, 2005). To estimate the near-surface dip angles for each fault branch, we performed a simple fault kinematics calculation based on comparison between horizontal shortening and vertical displacement across the faults. We compiled the 1998–2006 leveling measurements yielding the vertical displacement, and the creep meter data and GPS data for the same period yielding the horizontal shortening. Assuming a semi-rigid block behavior, the dip angle of the fault can be determined from the ratio of horizontal and vertical displacement.

Because the creep meters are not precisely perpendicular to the strike of the fault and the fault moved obliquely with respect to fault strike, we calibrated this horizontal displacement based on the shortening amount (L) of creep meter and its geometrical relationship with the trends of creep meter (θ_c), the trend of profile (θ_p) and fault relative motion (θ_m), as shown below.

$$\text{Horizontal relative displacement (H)} = L \times \frac{\cos(\theta_m - \theta_p)}{\cos(\theta_m - \theta_c)}$$

For θ_c, the creep meters C3, C4 and C5 trend N115°E, N156°E, and N164°E, respectively. The general trend of the Chihshang fault in the Chihshang area is N20°E, so that the profile perpendicular to the fault (θ_p) has a trend of N110°E. Regarding the vector of fault relative motion (θ_m), we considered a few possibilities based on different geodetic results and models. First, a vector N326°E of relative motion has been yielded from the rigid block model (Lee and Angelier, 1993) based on the 1983–1985 trilateration network across the Longitudinal Valley in the Chihshang area (Yu and Li, 1989). Second, the 2003–2005 GPS measurements on the near-fault networks (Lee et al., 2006) indicate that the motion of the hangingwall with respect to the footwall during the Chengkung earthquake trends N310°E at Chinyuan site. On the other hand, the far-field GPS data indicated a motion vector of about N325°E for fault during the same period (Lee et al., 2006). Because we are interested in the shallow fault geometry and its kinematics, we adopted the near-fault GPS vectors from 2003–2005. Consequently, we used a motion vector of N310°E.

For the leveling data, we used benchmark I of the Chinyuan site (Fig. 4) as the reference point, which is located in the footwall and is the same as for the near-fault GPS vector estimation. The 1998–2006 Chinyuan leveling route with 15 benchmarks followed the river bank of the Chinyuan River for a distance of about 250 m across the fault (Fig. 8). Based on these annual repeated leveling measurements, we plotted the accumulative elevation changes (V) for all benchmarks of the Chinyuan site with respect to benchmark I, quantifying the vertical displacement across each fault branch (Fig. 9). The dip angles for each branch fault, α_{T1}, α_{T2} and α_B that correspond to the three branches beneath creep meters C3, C4 and C5 respectively, can thus be determined by plotting the accumulative vertical and horizontal displacements for each of them (Table 1; Fig. 9).

The dip angle of the deeper part of the main fault beneath the shallow-level flower structure, α_{MT}, was estimated by the difference between the two benchmarks outside of the pop-up, that is, the benchmarks I and A (Figs. 4 and 8). Because campaigned GPS

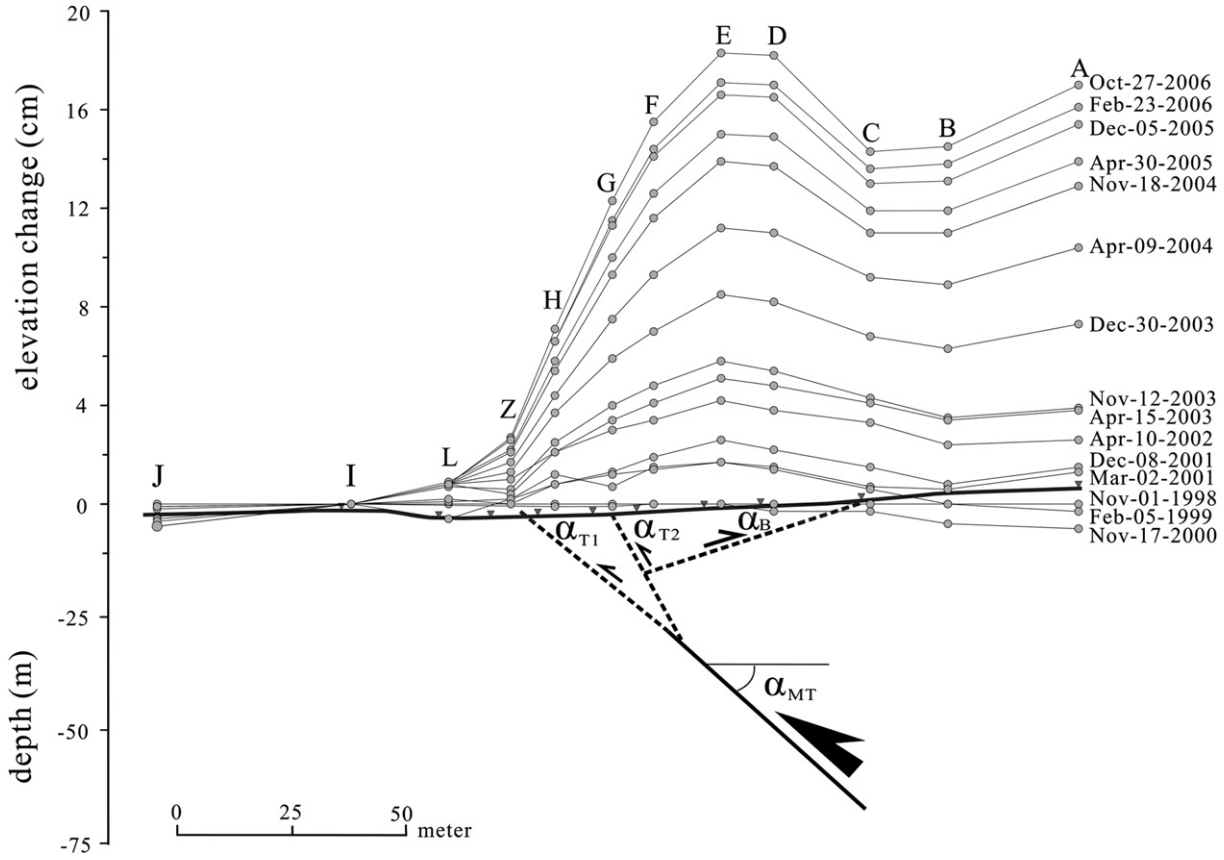

Fig. 8. Schematic 2-D subsurface fault geometry and the related leveling results at the Chinyuan site from 1998 to 2006. A–J: leveling benchmarks. The elevation changes for each benchmark were calculated with respect to the benchmark I. Note that the leveling data show a pop-up structure bounded by the three-branch fault system.

measurements were conducted at these two particular benchmarks since 2003, we adopted the GPS vectors and projected to horizontal shortening perpendicular to the fault strike. By plotting the horizontal shortening versus vertical displacements, we obtained a linear trend for dip angle of approximate 42° for the main fault (α_{MT}) (Fig. 9d). For the dip angle of each branch fault, we used two paired benchmarks across the surface trace of each branch for estimation. For instance, benchmarks I and H were selected for the sub-fault under creep meter C3, H and F under creep meter C4, and C and D under creep meter C5. We obtained the fault dip angles of 42°±4° and 34°±2° for α_{T1}, and 60°±1° and 65°±2° for α_{T2}, 16°±1° for α_B (Fig. 9). By extrapolating the fault branches down-dip, we place the bottom of the pop-up structure at about 30–40 m below the surface (Fig. 8). The ^{14}C dating from the T2 core showed a depositional age of 1800 ± 150 BP at the depth of 20 m. It meanshis pop-up structure is relatively young and has been developing at shallow depth within the Chinyuan alluvial fan during the last few thousand years.

5. Ages constraints and uplifted alluvial deposits

5.1. Trench age analysis

As mentioned above, three trenches in Chinyuan were excavated across the main fault scarp (Chu, 2007). The trenches Tch-I and Tch-II in Chinyuan alluvial fan showed a gentle anticlinal fold in the uppermost 8 m of sediments, which are unconformably covered by recent soil. On the other hand, the trench in southern Chinyuan (Tch-III) showed two young faults, possibly related to the 1951 and 2003 earthquakes, in addition to anticlinal fold (Chu, 2007). Also, in the upper 3 m, several fault branches are present with rather low dip angles. The radiometric dates in the Chinyuan trenches indicate the ages of 200–300, 500–600 yr and 900 yr BP at the depths of about 2 m, 4 m and 9–10 m, respectively. We thus obtained the alluvial sedimentation rate of about 1 cm per year for the last 1 thousand years.

5.2. Borehole age analysis

In the T2 borehole, two radiometric ^{14}C ages of 1640–1720 yrs and 1760–1840 yrs were determined at depths of 12.3 m and 20.7 m (Chen, personal comm.). We thus obtained average sedimentation rates of 0.7 cm/yr, 1.2 cm/yr, and 7 cm/yr for the periods of 1680 yr BP to present, 1800 yr BP to present, and from 1680 to 1800 yr BP, respectively. Because the T2 core is located within the channel of the Chinyuan River, we interpret the sedimentation rate for the alluvial deposit to have averaged about 1 cm/yr during the past 2 thousand years, although the sedimentation rate was not constant through this time span. As we observed in the field, the rivers from the Coastal Range can yield deposits that are several meters thick and coarse-grained during typhoon events. Nevertheless, extrapolating the 1 cm/yr rate to the 60-m-long T2 core, we obtain at least 6 thousand years of alluvial deposits in the Chinyuan River channel.

Considering the present interseismic uplift rate of about 0.4 cm/yr, 0.3 cm/yr, and 0.3 cm/yr across the surface C3 fault, C4 fault, and C5 fault from the leveling measurements (Lee et al., 2006), it is difficult to produce the surface scrap in the northern part of the Chinyuan village, where three branches distribute in the channel (i.e., stream power would erode the surface scarps) and the alluvial deposits of the Chinyuan River (i.e., the deposits would bury the surface scarps). By contrast, the surface fault scarp is preserved in the southern part of the Chinyuan, where the three branches merge

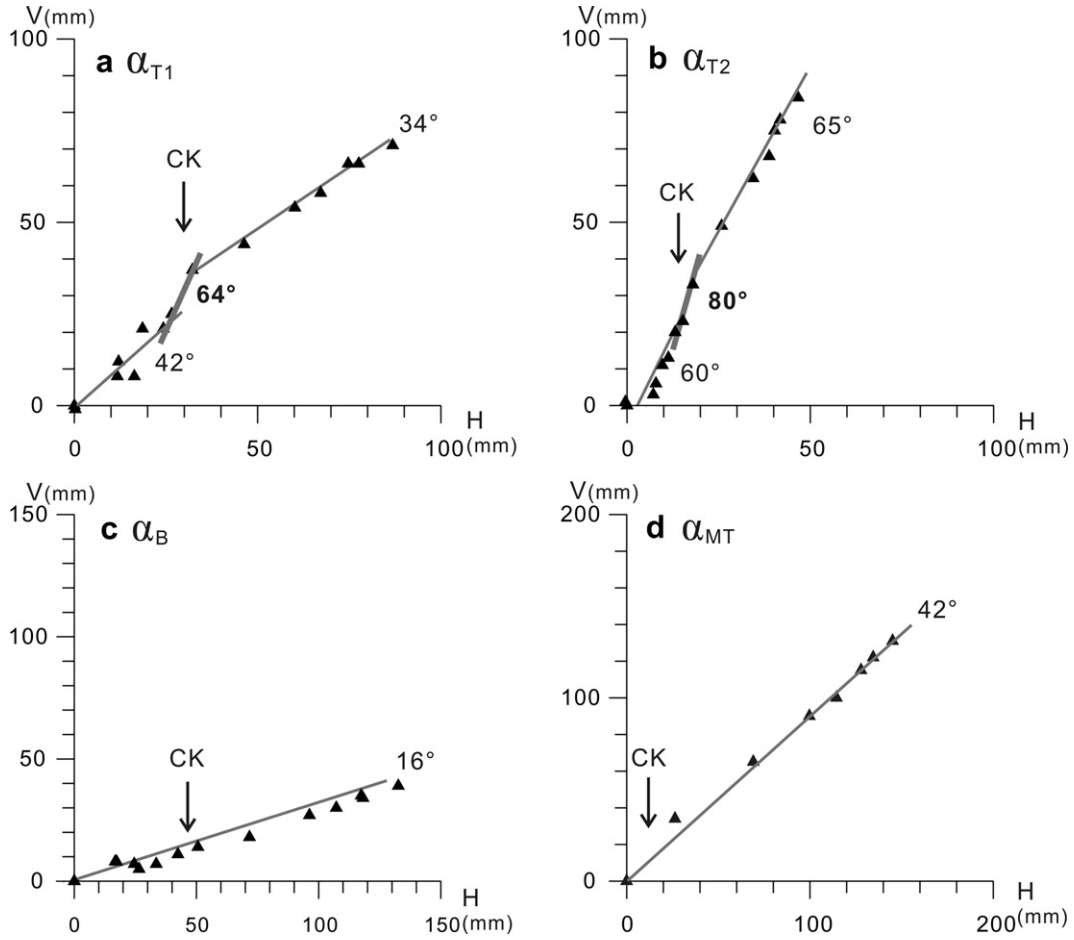

Fig. 9. Diagrams of accumulative vertical displacements (V) versus horizontal displacements (H) for the three branches (a) C3 (b) C4 (c) C5, and (d) the main fault. The vertical displacements derived from bi-annual leveling measurements from 1998 to 2006. The horizontal displacements derived from creep meter recording (1998–2006) for three branches and from GPS measurements (2002–2006) for the underlying main fault. CK: the 2003 Chengkung earthquake. See detailed explanations in the text.

into one single fault outside of the present Chinyuan River channel. The leveling measurements indicated a relative uplift rate of about 2.0 cm/yr across the scarp near trench Tch-III and core T3, which is significantly greater than the 1 cm/yr sedimentation rate yielded from the Trench Tch-III. As a result, it is favorable for developing a geomorphic fault scarp in the single-fault zone.

Table 1
Accumulative vertical displacements (V) versus horizontal displacements (H) across C3, C4 and C5 fault at Chinyuan site from 1998 to 2006. Vertical displacement derived from leveling measurements and horizontal one from creep meters recordings. Horizontal displacements of the main fault derived from the result of GPS from 2003 to 2006.

Date	C3 fault		C4 fault		C5 fault		Main fault	
	H(mm)	V(mm)	H(mm)	V(mm)	H(mm)	V(mm)	H(mm)	V(mm)
Nov-1998	0	0	0	0	0	0		
Feb-1999	0	−1	0	1	0	0		
Nov-2000	11.	8	8	6	18	8		
Mar-2001	11	12	7	3	17	8		
Dec-2001	15	8	10	11	25	7		
Apr-2002	17	21	11	13	27	5		
Apr-2003	22	21	13	20	35	7		
Nov-2003	25	25	15	23	44	11	0	0
Jan-2004	30	37	18	33	52	14	26	34
Apr-2004	44	44	26	49	74	18	69	65
Nov-2004	57	54	35	62	99	27	100	90
Apr-2005	63	58	39	68	110	30	114	100
Nov-2005	71	66	41	75	121	35	128	115
Feb-2006	73	66	42	78	122	34	134	122
Oct-2006	82	71	47	84	137	39	145	131

In the Wan-I borehole, the main fault is interpreted to occur at the depth of 29 m. Below the main fault, the footwall is composed of alluvial deposits of the Longitudinal Valley rivers with two radiometric ^{14}C ages of 4090–4390 yrs and 5600–5990 yrs from depths of 44 m and 68 m, respectively (Chu, 2007). One obtains average footwall deposition rates of 1.2 cm/yr for the periods of 5795 yr BP to present, with a variation of 1.0 cm/yr and 1.6 cm/yr from 4240 yr BP to present and from 4240 to 5795 yr BP, respectively. Again, this long-term sedimentation rate of 1.2 cm/yr in the footwall for the last 6 thousand years is significantly slower than the present relative uplift rate of about 2.0–2.7 cm/yr revealed by the leveling data near the Wanan boreholes site (Yu and Liu, 1989). Consequently, several levels of Holocene terrace risers with a terrace height of a few meters to tens of meters occur in the hangingwall in the Chihshang area (Chu, 2007; Liu et al., 2009).

5.3. Terrace age analysis

A few terraces risers were previously dated in the study area from Fuli to Wanan (Chu, 2007), allowing us to discuss the evolution of the Chihshang fault in the late Quaternary and in particular the Holocene time. The CY2 terrace, a Chinyuan River terrace about 300 m east of the surface fault trace (Fig. 4a) has about 15 m of terrace height as measured with respect to the river bed, and is about 30 m higher than the similar deposits in the footwall close to the scarp downstream of the Chinyuan River. Considering the ^{14}C age of 530–650 yr BP determined on top of the CY2 terrace and the

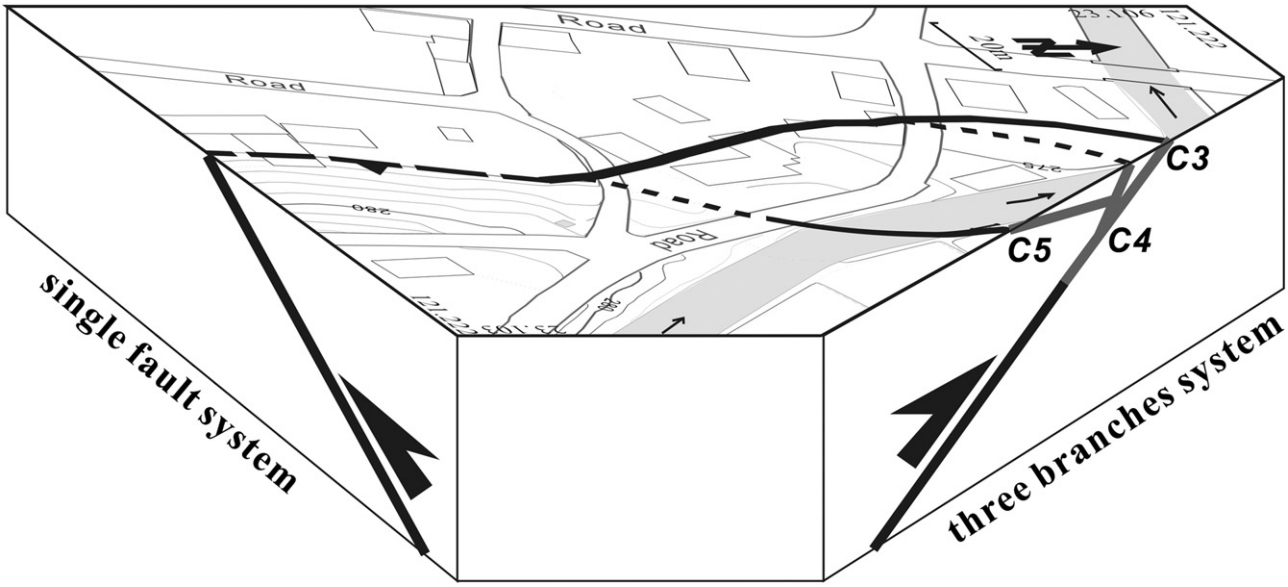

Fig. 10. Fault architecture at Chinyuan. 3-D perspective view shows the three-branch fault system developed mainly within the alluvial fan of the Chinyuan River. Outside of the Chinyuan River fan, the Chihshang fault shows a single fault system.

identical age determined in the trench Tch-III, we correlate the CY2 terrace with the fluvial deposits in Tch-III trench. The deposits in the hangingwall terrace have been uplifted with respect to the footwall borehole. Assuming that the slope of Chinyuan River profile remained relatively stable during the past 600 years, it indicates 27 m of vertical difference in river profile from the CY2 site to the downstream fault scarp. We attribute the difference in height between the present vertical relief and the height difference between the datum in the footwall and hangingwall to fault movement. Adding that the 600-year sediments are found at the depth of 4 m in Trench Tch-III, we obtain the uplift rate of the CY2 terrace to be 2.1–3.6 cm/yr in the past 600 years.

We then considered three other terraces near the Chihshang fault that were dated by ^{14}C technique: FNC, FC, and SG (Chen, 2009). SG was dated to be 290–490 yr BP with a terrace height of 13–15 m; FC was dated to be 940–1080 yr BP with a terrace height of 25–27 m; and FNC was dated to be 6280–6410 yr BP with a terrace height of 48–50 m. River terraces near the Chihshang fault have been previously interpreted with two origins (Chu, 2007; Liu et al., 2009): one is as terraces of the rivers flowing along the Longitudinal Valley (e.g., SG, FC) and the other is as terraces of the smaller rivers flowing from the Coastal Range to the Longitudinal Valley (e.g., CY2, FNC). With these data, we calculated the relative uplift rates for each dated terrace: 2.2 cm/yr for SG, 2.4 cm/yr for FC, and 0.75 cm/yr for FNC. The estimated rates during the last 1 thousand years are generally compatible with the present-day value of 2–3 cm/yr derived from the leveling measurements during the last 20 years. However, the highest terrace (i.e., FNC, 6345 yr BP) reveals a much slow rate of relative uplift (0.75 cm/yr), suggesting that the fault movement might be significantly slower about 1–6 ka ago as compared to the present, or that the terrace might be contaminated by colluviums deposits from nearby hills. Further work is needed to select between these two hypotheses.

6. Conclusion

1. Based on field investigation we mapped the detailed surface-rupture of the Chihshang fault at the Chinyuan site of the Chihshang Active Fault Observatory in eastern Taiwan. Compared to one single fault, the Chihshang fault has three branches, two west-vergent thrusts and a backthrust at the Observatory (Fig. 10). We found that the fault branches occurred exclusively within the alluvial fan of the Chinyuan River, implying a possible correlation between the fault branches development and these unconsolidated deposits.
2. The geological strata are mainly occupied by the fluvial deposits of the Chinyuan River and the rivers from the Central Range at the Observatory. Based on three borehole cores analysis, we reconstructed geological cross sections across the Chihshang fault. At the near-surface level, we interpret the east-dipping main fault to develop into a diffused zone composed of several small faults, instead of a sharp fault plane. These three major branches are coupled with a 50–60-m wide pop-up structure in the upper 30–40 m unconsolidated young gravel layers, which were deposited during the last 3000–4000 yrs BP, based on the ^{14}C dating. This gentle pop-up in the young alluvial gravels is interpreted to be associated with the hangingwall folding of the Chihshang fault, based on observations in the subsurface excavation and leveling measurements.
3. Combining the 1998–2006 repeated measurements on dense geodetic network at the Chinyuan site, notably the leveling, creep meter and GPS, we completed a kinematic analysis and evaluated the dip angles of the Chihshang fault including each surface branches at the shallow level. We obtained (1) the frontal branch fault with a dip angle of 34–42°, which corresponds to surface main geomorphic scarp, (2) the middle branch fault, about 10–15 m east of the frontal branch, with greater dip angle of about 60–65°, (3) the west-dipping backthrust with a very gentle dip of 16°. Beneath this pop-up structure, the main fault was estimated to have a dip angle of about 42°.
4. Compiling the age data for river terraces we obtain a long-term relative uplift rate of 2.2–2.4 cm/yr in the hangingwall of the Chihshang fault for the past 1 thousand years, which generally is in an agreement, although a little smaller, with short-term leveling measurements. Based on the age data from trenches, borehole cores and river terraces, we also estimated the sedimentation rate of alluvial deposits across the Chihshang fault. We obtain an average sedimentation rate of 1.2 cm/yr for the Chinyuan River in the past 2 thousand years and an average

sedimentation rate of about 1.0–1.2 cm/yr for the Longitudinal Valley rivers in the past six thousand years.

Acknowledgments

We are grateful for the comments and suggestions of Editor William Dunne and two reviewers. Our work was conducted within the France-Taiwan cooperation framework (Institut Français à Taipei and National Science Council of Taiwan). The research was supported by Institute of Earth Sciences, Academia Sinica, National Central University and National Science Council (grants NSC99-2116-M-001-006, NSC98-2116-M-001-011, NSC98-2116-M-008-004, NSC97-2116-M-001-002, NSC96-2116-M-008-006 and NSC97-2745-M-008-017) and the Institut Universitaire de France regarding the second author. We sincerely thank Mr. Jiang Guo-Chang, Mr. Chang Shern-Hsiung and many assistants and students, who supplied generous helps during our field work. This is a contribution of Institute of Earth Sciences, Academia Sinica, IESAS-1541.

Appendix. Supplementary data

Supplementary data associated with this article can be found in on-line version at doi:10.1016/j.jsg.2011.01.015.

References

Angelier, J., 1986. Geodynamics of the Eurasia – Philippine Sea plate boundary: preface. Tectonophysics 125 (13), 9–10.
Angelier, J., Chu, H.-T., Lee, J.-C., 1997. Shear concentration in a collision zone: kinematics of the Chihshang Fault as revealed by outcrop-scale quantification of active faulting, Longitudinal Valley, eastern Taiwan. Tectonophysics 274, 117–143.
Angelier, J., Chu, H.-T., Lee, J.-C., Hu, J.-C., 2000. Active faulting and earthquake risk: the Chihshang Fault case, Taiwan. Journal of Geodynamics 29, 151–185.
Barrier, E., Muller, C., 1984. New observations and discussion on the origin and age of the Lichi Mélange. In: Memoir of the Geological Society of China, vol. 6 303–326.
Biq, C. 1973. Kinematic pattern of Taiwan as an example of actual continent-arc collision. Report of the Seminar on Seismology. US–ROC Cooperative Science Program 25, pp. 149–166.
Chang, C.-P., Angelier, J., Huang, C.-Y., 2000. Origin and evolution of a melange: the active plate boundary and suture zone of the Longitudinal Valley, Taiwan. Tectonophysics 325, 43–62.
Chang, S.-H., Wang, W.-H., Lee, J.-C., 2009. Modeling surface creep of the Chihshang Fault in eastern Taiwan with velocity-strengthening friction. Geophysical Journal International 176 (2), 601–613.
Chen, H.-Y., Yu, S.-B., Kuo, L.-C., 2006. Coseismic and postseismic surface displacements of the 10 December 2003 (Mw 6.5) Chengkung, eastern Taiwan, earthquake. Earth, Planet and Space 58, 5–21.
Chen, W.-S., 1991. Origin of the Lichi Mélange in the Coastal Range, eastern Taiwan. In: Central Geological Survey, Special Publication, vol. 5 257–266.
Chen, W.-S., 1997. Lithofacies analyses of the arc-related sequence in Coastal Range, eastern Taiwan. In: Journal of the Geological Society of China, vol. 40 313–338.
Chen, W.-S. 2009. The fault slip long term velocity and recurrence period. Report of Central Geological Survey, pp. 31–40.
Cheng, S.-N., Yeh, Y.-T., Yu, M.-S., 1996. The 1951 Taitung earthquake in Taiwan. In: Journal of the Geological Society of China, vol. 39 (3), 267–285.
Chu, H.-T., Lee, J.-C., Angelier, J. 1994. Non-seismic rupture of the Tapo and the Chinyuan area on the southern segment of the Huatung Longitudinal Valley Fault, Eastern Taiwan. Annual meeting of the Geological Society of China, Taipei, pp. 1–5.
Chu, Y.-K. 2007. Paloseismology of the Chihshang Fault (in Chinese with English abstract), Master Thesis. National Taiwan University, pp. 110.
Ernst, W.G., 1977. Olistostromes and included ophiolitic debris from the Coastal Range of eastern Taiwan. In: Memoir of the Geological Society of China, vol. 2 97–114.
Ho, C.-S., 1986. Asynthesis of the geologic evolution of Taiwan. Tectonophysics 125, 1–16.
Hsu, K.-J., 1988. Malange and the mélange tectonics of Taiwan. In: Proceedings of the Geological Society of China, vol. 32 82–87.
Hsu, T.-L., 1962. Recent faulting in the longitudinal valley of eastern Taiwan. In: Memoir of the Geological Society of China, vol. 1 95–102.
Hsu, Y.-J., Yu, S.-B., Chen, H.-Y., 2009. Coseismic and postseismic deformation associated with the 2003 Chengkung, Taiwan, earthquake. Geophysical Journal International 176 (2), 420–430.
Hu, J.-C., Cheng, L.-W., Chen, H.-Y., Wu, Y.-M., Lee, J.-C., Chen, Y.-G., Lin, K.-C., Rau, R.-J., Kuochen, H., Chen, H.-H., Yu, S.-B., Angelier, J., 2007. Coseismic deformation revealed by inversion of strong motion and GPS data: the 2003 Chengkung earthquake in eastern Taiwan. Geophysical Journal International 169, 667–674.
Huang, C.-Y., Yuan, P.-B., Tsao, S.-J., 2007. Temporal and spatial records of active arc-continent collision in Taiwan: a synthesis. In: Geological Society of America, vol. 118 274–288.
Kuochen, H., Wu, Y.-M., Chen, Y.-G., Chen, R.-Y., 2007. 2003 Mw6.8 Chengkung earthquake and its related seismogenic structures. Journal of Asian Earth Sciences 31 (3).
Lee, J. C. 1994. Structure et déformation active d'un oroge`ne: Taiwan, Mem. Sc. Terre 94-17 thesis, 281 pp., Univ. Pierre et Marie Curie, Paris.
Lee, J.-C., Angelier, J., 1993. Localisation des déformations actives et traitement des données géodésiques: l'exemple de la faille de la Vallée Longitudinale, Taiwan. Bulletin de la Société géologique de France 164 (4), 533–540.
Lee, J.-C., Angelier, J., Chu, H.-T., Hu, J.-C., Jeng, F.-S., 2001. Continuous monitoring of an active fault in a plate suture zone: a creepmeter study of the Chihshang active fault, eastern Taiwan. Tectonophysics 333 (1–2), 219–240.
Lee, J.-C., Angelier, J., Chu, H.-T., Hu, J.-C., Jeng, F.-S., Rau, R.-J., 2003. Active fault creep variations at Chihshang, Taiwan, revealed by creepmeter monitoring. Journal of Geophysical Research 108 (B11), 2528.
Lee, J.-C., Angelier, J., Chu, H.-T., Hu, J.-C., Jeng, F.-S., 2005. Monitoring active fault creep as a tool in seismic hazard mitigation. Insights from creepmeter study at Chihshang, Taiwan. Comptes Rendus Geosciences 337, 1200–1207.
Lee, J.-C., Chu, H.-T., Angelier, J., Hu, J.-C., Chen, H.-Y., Yu, S.-B., 2006. Quantitative analysis of co-seismic surface faulting and post-seismic creep accompanying the 2003, Mw = 6.5, Chengkung earthquake in eastern Taiwan. Journal of Geophysical Research 111 (B02405).
Liu, Y.-C., Lee, J.-C., Chen, R.-F., 2009. The Holocene strath terraces of the longitudinal valley at Chihshang in eastern Taiwan and its implication to the activity of the Chihshang fault. Eos Transactions of American Geophysical Union 90 (52) Fall Meet. Suppl., Abstract T33B-1893.
Marone, C.J., Scholz, C.H., Bilham, R., 1991. On the mechanics of earthquake afterslip. Journal of Geophysical Research 96, 8441–8452.
Page, B.M., Suppe, J., 1981. The Pliocene Lichi Mélange of Taiwan: it's plate-tectonic and olistostromal origin. American Journal of Science 281, 193–227.
Perfettini, H., Avouac, J.-P., 2007. Modelling afterslip and aftershocks following the 1992 Landers earthquake. Journal of Geophysical Research 112. doi:10.1029/2006JB004399.
Sieh, K., Stuiver, M., Brillinger, D., 1989. A more precise chronology of earthquakes produced by the San Andreas Fault in southern California. Journal of Geophysical Research 94, 603–623.
Sieh, K., Williams, P., 1990. Behavior of the southernmost San Andreas Fault during the past 300 years. Journal of Geophysical Research 95, 6629–6645.
Teng, L.-S., Wang, Y., 1981. Island arc system of the Coastal Range, eastern Taiwan. In: Proceedings of the Geological Society of China, vol. 24 99–112.
Thatcher, W., 1984. The earthquake deformation cycle, recurrence, and the time-predictable model. Journal of Geophysical Research 89, 5674–5680.
Tsai, Y.-B., 1986. Seismotectonics of Taiwan. Tectonophysics 125, 17–37.
Wu, Y.-M., Chen, Y.-G., Shin, T.-C., Kuochen, H., Hou, C.-S., Hu, J.-C., Chang, C.-H., Wu, C.-F., Teng, T.-L., 2006. Coseismic versus interseismic ground deformations, fault rupture inversion and segmentation revealed by 2003 Mw 6.8 Chengkung earthaquake in eastern Taiwan. Geophysical Research Letters 33, L02312. doi:10.1029/2005GL024711.
Yu, S.-B., Chen, H.-Y., Kuo, L.-C., 1997. Velocity field of GPS stations in the Taiwan area. Tectonophysics 274, 41–59.
Yu, S.-B., Jackson, D.D., Yu, G.-K., Liu, C.-C., 1990. Dislocation model for crustal deformation in the Longitudinal Valley area, eastern Taiwan. Tectonophysics 183, 97–109.
Yu, S.-B., Kuo, L.-C., 2001. Present-day crustal motion along the Longitudinal Valley Fault, eastern Taiwan. Tectonophysics 333, 199–217.
Yu, S.-B., Liu, C.-C., 1989. Fault creep on the central segment of the longitudinal valley fault, Eastern Taiwan. In: Proceedings of the Geological Society of China, vol. 32 (3), 209–231.